International Journal of Applied Pharmaceutics

ISSN- 0975-7058 Vol 17, Issue 1, 2025

Original Article

DESIGN, DEVELOPMENT, AND CHARACTERIZATION OF CURCUMIN-LOADED NANO TABLET IN ENDOMETRIOSIS TREATMENT

UMMANGALBALAN ABHINI[2], GURUSAMY MARIAPPAN[2], BHAVNA KUMAR[1*]

[1]Faculty of Pharmacy, DIT University, Dehradun, Uttarkhand, India. [2]St Mary's College of Pharmacy, Secunderabad, Telangana-500025, India

[*]Corresponding author: Bhavna Kumar; [*]Email: bhavnano@gmail.com

Received: 31 Aug 2024, Revised and Accepted: 11 Nov 2024

ABSTRACT

Objective: The goal was to simplify the manufacture of curcumin-loaded-nanosponges (CUNS) and test their vaginal delivery of CU for endometriosis in mice.

Methods: The independent parameters of CU-β-Cyclodextrin (CU-β-CD) NS generation were improved using box-behnken design (BBD). BBD with three factors and three levels was used for the studies. The study used carbonyldiimidazole as a cross-linking agent and lyophilization to create CU-β-CDNS. The anti-endometriosis activity of nano-tablet was tested in mice with peritoneal endometriosis.

Results: The mean particle size was 76.78–154.56 nm, and the encapsulation effectiveness was 76.62–86.68%. Transmission Electron Microscopy showed that the polymer encapsulated CU. *In vitro* antioxidant activity showed that CU and CUNS had SC_{50} values of 5243.52±389.92 and 187.36±16.78 µg/ml, respectively. Bio-adhesion studies showed hydroxypropyl methylcellulose and xanthan gum performed better. The F1 and F2 formulations had better *in vitro* drug release at 12 h, with values of 97.12±2.38 and 95.34±3.24%, respectively. Photostability and simulated intestinal fluid testing were good. Endometriosis mice had leukocyte infiltration and fibrosis, while control mice had increased stromal vessel density and intact epithelium. However, CU nanogel greatly alleviated these issues. Histopathology demonstrated CUNS-pill corrected endometrial pathology.

Conclusion: The study advised CUNS-pill for endometriosis treatment.

Keywords: Endometriosis, Nanosponges, Cyclodextrins, Curcumin, Box-behnken design, Histopathology

DOI: https://dx.doi.org/10.22159/ijap.2025v17i1.52533 Journal homepage: https://innovareacademics.in/journals/index.php/ijap

INTRODUCTION

Pelvic comfort and pregnancy can be severely compromised by endometriosis, which causes tissue that mimics the uterine lining to develop outside the uterus. 20% to 50% of infertile women suffer with endometriosis, according to the American society of reproductive medicine. The most effective method for restoring fertility after cyst and scar tissue removal is surgical removal [1]. As a result of acute pain, fatigue, depression, anxiety, and infertility, it might reduce quality of life. That is why endometriosis treatment is so important [2]. As a result, herb endometriosis treatment is becoming more popular. Studies on the potential medicinal uses of plant and dietary components are underway for the treatment of cancer, a benign condition that shares certain symptoms with endometriosis [3].

Curcumin (CU) appears to be responsible for turmeric's anti-oxidant, anti-inflammatory, anti-mutagenic, anti-viral, anti-fungal, and anti-carcinogenic properties [4]. CUtreatment dramatically reduced IL-1ß and NF-κB production in human endometrial stromal cells [5]. CU influences the regulation of inflammatory mediators like TNF-α and TGF-ß1. The current study was aimed to release CU at the target site; however, all the conventional delivery systems are not able to deliver the therapeutics to the target site. Hence, it is essential to develop sophisticated delivery systems to treat endometriosis.

There are numerous drug-loaded nanoparticles designed to overcome delivery difficulties. Numerous investigations have demonstrated that nanosponges (NS) improves pharmaceutical targeting and bioavailability [6, 7]. The sponge acts as a three-dimensional network or scaffold, and it is spread in a matrix containing lubricants, diluents, anti-caking agents, and excipients suitable for producing tablets or capsules for vaginal delivery [8, 9]. β-CD based NS (β-CDNS) is a new and novel option for pharmaceutical formulations [10].

Response Surface Methodology (RSM) is a statistical tool used in Design of Experiments (DoE) [11, 12]. In response surface modelling, Box-Behnken Design (BBD) and CCD (Central Composite Design) are the two most used designs [13]. Incorporating CU into neural scaffolds and delivering it to the target site (the endometrial area) is the major objective. The study's originality and rationale lie in its goal of creating a CU-graded formulation within the nanoparticle range and delivering the active ingredient to the endometrium on purpose. Due to the site-specific nature of the disease, traditional dose forms (such as oral solid dosage forms like tablets and capsules) may not produce the desired therapeutic results. The best option here would be an intravaginal formulation. Furthermore, the most effective and suitable method of purposefully delivering the active medication to the endometrium is via intravaginal nano formulation. Therefore, this may be an excellent strategy for endometriosis treatment.

MATERIALS AND METHODS

Materials

β-CD was procured from Gangwal Chemicals Pvt. Ltd. Mumbai, India. The chemical 2-Diphenyl-1-picrylhydrazyl and carbonyldiimidazole were obtained from Sigma Aldrich Mumbai, India. Analytical-grade materials and reagents were utilised in the investigation. CU was procured from Naturita Agro Products Ltd. (Hyderabad, India).

Methods

Design of experiments

CUNS were synthesised using BBD, which included three independent variables: solvent volume (C), stirring speed (A), and stirring duration (B). BBD used a three-factor, three-level approach to optimise and assess the effects of factors on interactive, quadratic response parameters. Second-order polynomial models were applied and proved beneficial in explaining quadratic response surfaces [14].

Synthesis of nanosponges

Cross-linked ß-CD-based NS were made with carbonyldiimidazole [15]. Add carbonyldiimidazole to anhydrous β-CD in

dimethylsulfoxide (DMSO) and reflux on an oil bath. The product was isolated after the reaction, washed, and extracted with ethanol for four hours. White powder was then dried at 60 °C. Water was used to dispose of the fine powder. Lyophilization removed water-suspended colloids.

Solubilization efficiency of nanosponges

According to literature, NS solubilisation efficiency was studied [16]. 1000 mg of CU was suspended in 10 ml water and centrifuged at 104 rpm to extract free CU. 10 ml of methanol was added to the supernatant to remove NS-encapsulated CU. The drug content in colloidal supernatant was measured by UV spectrophotometer.

Fabrication of CU-β-CDNS

Lyophilization produced CUNS. The 500 mg NS was dissolved in 100 ml of water. Add 500 mg CU and sonicate for 20 min. For 20 min, the suspension was centrifuged at 2000 rpm. Separate and freeze-dry the colloidal supernatant at-20 °C using lyophilization. Dry powder from lyophilization was stored in a desiccator [17].

Data analysis

P value, R^2 adjusted, and lack of fit were used to find the best model. Coefficient of variation and R^2. Data with P values over 0.005 are removed from the model. As seen in the equation below, multiple regression analysis can analyse each response parameter using a quadratic model.

$$Y = \beta_0 + \beta_1 X_1 + \beta_2 X_2 + \beta_3 X_3 + \beta_{12} X_1 X_2 + \beta_{23} X_2 X_3 + \beta_{13} X_1 X_3 + \beta_{11} X_1^2 + \beta_{22} X_2^2 + \beta_{33} X_3^2$$

Where,

Y–Response parameter

β_0– Intercept

β_1– β_3– Regression coefficients

β_{12}, β_{13} and β_{23}– Interaction coefficients

β_{11}, β_{22} and β_{33}– Quadratic coefficients

X_1, X_2 and X_3– Main influencing factors

X_1X_2– Interactive effect

X_1^2, $X_2^2$and X_3^2– Quadratic effect

Backward elimination technique eliminates independent variables that don't affect the regression equation. 3D response surface showed independent variable-response association [18].

Characterisation of plain β-CDNS and CUNS

Plain β-CDNS and CUNS were analysed for their entrapment efficiency (EE), percent drug loading in NS, Particle Size (PS) [19], Polydispersity Index (PDI), Zeta Potential (ZP), Transmission Electron Microscopy (TEM), Fourier Transform Infrared Spectroscopy (FTIR), Differential Scanning Calorimetry (DSC), X-ray Powdered Diffraction (XRPD) and *In vitro* release of drug from NSformulations [20], Photo Stability Studies [21], Simulated Intestinal Fluid (SIF) Stability Assay [22].

Preparation of nano tablet

Direct compression produced CU-containing vaginal tablets. A 10-station tablet machine with flat-faced 12 mm punches generated 500 mg of 100 mg CU tablets. A particle size of less than 160 µm was maintained to prevent fractional segregation and provide a homogeneous mix before compression [23].

Physical characterization of tablets

Quality control factors of tablets such as thickness, hardness, weight fluctuation, friability, swelling capacity [24], *ex-vivo* mucoadhesion time [25], *in vitro* bioadhesion, and *in vitro* CU release studies were investigated.

Evaluation of anti-endometriosis activity of CU nano tablet in mice model

Induction of peritoneal endometriosis in BALB/cmice

Animal studies were conducted out in accordance with the institute's Animal Ethics Committee requirements. Peritoneal endometriosis was induced using Somigliana *et al.*'s technique [26], with slight modifications. In total, 30 female adult BALB/c mice aged 6-8 w were used in tests. Here, 5 mice were kept as donor animals (n=5), while the remaining 25 were separated into 5 groups (n=5). Group 1: Normal Control, Group 2: endometriosis control, Group 3: typical tablet, Group 4: Nano tablet and Danazole is a group 5 standard medication. On day 0, donor mice were anaesthetised (ketamine 12 mg/kg body wt.) and slaughtered for sterile uterine horns. The endometrium was carefully removed, cut, suspended in sterile phosphate buffer saline (PBS), and inoculated into recipient mice's peritoneal cavities. Other groups were in 14-day administration treatment except normal control. The mice received 14 days of medication treatment after a week. The normal control mice received simply PBS (pH-7.4). No endometrial fragments were administered. Only PBS (0.6 ml) was used to record endometriosis control for 14 days. Danazole 100 mg/kg body weight (bwt), nanotablet 500 mg/kg bwt, and regular tablet 100 mg/kg bwt were given. Solid dose forms were dissolved in PBS and given intravaginally. To assess endometriosis protection, the above medications were given intravaginally daily for 15 days. After medication therapy, mice were slaughtered and their uteruses were processed for analysis.

Tissue extraction

A tissue suspension in PBS with protease inhibitors was minced at 4 °C. PBS extracts were obtained from the suspension after 15 min of 12,000 g centrifugation. The pellet was extracted in lysis buffer (10 mm Tris-HCl, pH 8.0,150 mm NaCl, 1% Triton X-100, and protease inhibitors) and centrifuged at 12,000 g for 15 min to produce Tx extracts.

Histopathological studies

Haematoxylin and eosin-stained 5 mm slices were made from samples after fixing and embedding in paraffin blocks. For dehydration, samples were prepared using ethanol. After cleaning with xylene and soaking in liquid paraffin wax at 58 °C, they were embedded in paraffin blocks. The samples were cut into 5 mm slices using a Rotary Microtome (Leica RM2255) and stained with MicromHMS7 and Haematoxylin and Eosin. The dyed slices were examined under an Olympus CX21 light microscope.

RESULTS AND DISCUSSION

Optimization of reaction conditions

The key process factors used for the synthesis of NS were namely reaction temperature, reaction time, stirring speed, and solvent volume. In this study, a Definitive screening design was used to screen the factors impact a significant effect on the practical yield and particle size of the NS. Reaction temperature and reaction played major effects on the practical yield. In addition, stirring speed and volume of the solvent are the significant factors affecting the particle size. Under ideal circumstances, this technique produced β-CDNS with a narrower particle size distribution and increased yield; these outcomes are in good accordance with the data examined by the design. In total, there were 13 runs in the experimental design, all of which were done at random to reduce the impact of outside variables. Table 1 displays the observed responses together with the design arrangement.

CU solubility in distilled water and NS solubilisation efficacy were compared. CU can be solubilised by NS (112 µg/ml). NS may be more soluble because they trap in the matrix and create an inclusion complex with the drug. In this work, solubilisation efficiency—the fundamental goal of NS synthesis-was increased. Based on BBD model provided by Design Expert® V 13.0.9.0, 17 model trials were randomly ordered and the dependent variable answers were presented in table 2.

Table 1: Definitive screening design and relative responses

Run	Factor 1	Factor 2	Factor 3	Factor 4	Response 1	Response 2
	A: Reaction temperature	B: Reaction time	C: Stitting speed	D: Volume of solvent	Practical yield	Particle size
Units	℃	min	rpm	ml	%	nm
1	90	480	3000	125	82.52	234.84
2	80	480	4000	100	78.18	162.78
3	100	540	4000	100	85.08	142.89
4	90	420	2000	100	91.58	301.56
5	100	420	3000	100	83.18	170.82
6	100	420	4000	150	83.56	138.12
7	80	420	4000	125	75.12	164.12
8	100	480	2000	150	83.22	356.78
9	90	540	4000	150	95.42	138.12
10	80	420	2000	150	73.56	341.89
11	80	540	3000	150	77.84	212.34
12	100	540	2000	125	82.24	362.72
13	80	540	2000	100	76.54	348.34

Table 2: Data of definitive screening design and relative responses

Run	Factor 1	Factor 2	Factor 3	Response 1	Response 2
	A: Stirring speed	B: Stirring time	C: Vol of solvent	PS	EE
Units	rpm	H	ml	Nm	%
1	4000	48	150	96.46	83.86
2	4000	24	150	110.34	81.82
3	3000	36	150	94.12	84.52
4	4000	36	200	107.78	79.56
5	2000	48	150	124.72	81.22
6	3000	36	150	93.48	83.92
7	3000	36	150	95.26	84.21
8	2000	36	200	144.12	76.62
9	2000	36	100	133.48	81.16
10	2000	24	150	154.56	79.34
11	3000	36	150	93.28	84.78
12	4000	36	100	99.12	82.12
13	3000	48	100	76.78	86.68
14	3000	24	200	108.56	81.12
15	3000	48	200	88.12	83.42
16	3000	24	100	101.44	83.89
17	3000	36	150	94.74	83.66

Table 3: ANOVA of quadratic model (mean particle size and encapsulation efficiency)

Source	Sum of squares	df	Mean square	F-value	p-value	
Model	6964.18	9	773.80	1545.03	<0.0001	significant
A-Stirring speed	2562.56	1	2562.56	5116.62	<0.0001	
B-Stirring time	986.12	1	986.12	1968.97	<0.0001	
C-Volume of solvent	178.23	1	178.23	355.86	<0.0001	
AB	63.68	1	63.68	127.15	<0.0001	
AC	0.9801	1	0.9801	1.96	0.2046	
BC	4.45	1	4.45	8.89	0.0205	
A^2	3154.64	1	3154.64	6298.80	<0.0001	
B^2	0.0033	1	0.0033	0.0066	0.9376	
C^2	0.7534	1	0.7534	1.50	0.2597	
Residual	3.51	7	0.5008			
Lack of fit	0.7223	3	0.2408	0.3460	0.7951	NS
Pure Error	2.78	4	0.6959			
Cor total	6967.69	16				
Source	Sum of Squares	df	mean Square	F-value	p-value	
Model	95.49	9	10.61	56.80	<0.0001	significant
A-Stirring speed	10.17	1	10.17	54.45	0.0002	
B-Stirring time	10.15	1	10.15	54.32	0.0002	
C-Vol of solvent	21.55	1	21.55	115.37	<0.0001	
AB	0.0064	1	0.0064	0.0343	0.8584	
AC	0.9801	1	0.9801	5.25	0.0558	
BC	0.0600	1	0.0600	0.3213	0.5885	
A^2	45.44	1	45.44	243.28	<0.0001	
B^2	1.66	1	1.66	8.87	0.0206	
C^2	4.80	1	4.80	25.70	0.0014	
Residual	1.31	7	0.1868			
Lack of Fit	0.5003	3	0.1668	0.8263	0.5442	Nonsignificant
Pure Error	0.8073	4	0.2018			
Cor total	96.79	16				

BBDs were utilised to optimise the affected variables based on early findings [27, 28]. Seventeen BBD three-factor and three-level trials were conducted. The mean PS (Y1) was 76.78–154.56 nm. EE (Y2) was 76.62–86.68. RSM methods reduce experimental runs and assess variable interactions. Analysing the data yielded regression coefficients, equations, and ANOVA values. Regression coefficient (R^2), analysis of variance, and lack of fit metrics were utilised to validate a second-order quadratic model that fit all the data. Table 3 demonstrate that quadratic models with the highest F values fit the data best.

Multiple linear regression analysis produced mathematical formulas for each of the three response variables. Positive correlations are synergistic, while negative correlations are antagonistic. Both regression equations were significant. The fitness of every quadratic model was confirmed by its non-significant lack of fit. All models' multiple regression analyses use coefficient of variation, adjusted R^2, and R^2 values. The model is appropriate because both response parameters have R^2 values over 0.98. A higher R^2 value does not always mean the model is suitable because other variable components contribute to it. Thus, the adjusted R^2 value and model adequacy must be assessed.

The Polynomial regression equation for mean particle size (Y_1) and encapsulation efficiency (Y_2) are 94.18–17.90 A-11.10 B+4.72 C+3.99 AB–0.49 AC+1.05 BC+27.37 A^2-0.02 B^2–0.42 C^2 and 84.22+1.13 A+1.13 B–1.64 C+0.04 AB+0.49 AC–0.12 BC–3.29 A^2+0.62 B^2– 1.07 C^2 respectively.

Mean particle size

Drug stability, solubility, dissolution, and tissue penetration depend on particle size distribution. The Nano formulation has 76.78–154.56 nm particles. Model significance was shown by f=1545.02. Model significance is shown by a P-value below 0.05. The F-value and P-value show that model terms A, B, C, AB, BC, and A^2 are significant. Lack of fit was not significant at an F-value 0.35. The adjusted R^2 value of 0.9988 and anticipated R^2 value 0.9977 revealed satisfactory model terms. Signal-to-noise ratio should exceed 4. The ratio of 143.084 indicates appropriate signal strength. You can browse the design area with this model. The equation shows that component C considerably increases particle size, whereas variables A and B decrease it. The individual effects plot and perturbation plot compare A, B, and C values by particle size in fig. 1(A) and 1(B). As seen in the fig. A has the greatest effect on particle size, while B has an intermediate effect. Fig. 1 shows how independent variables affect practical yield.

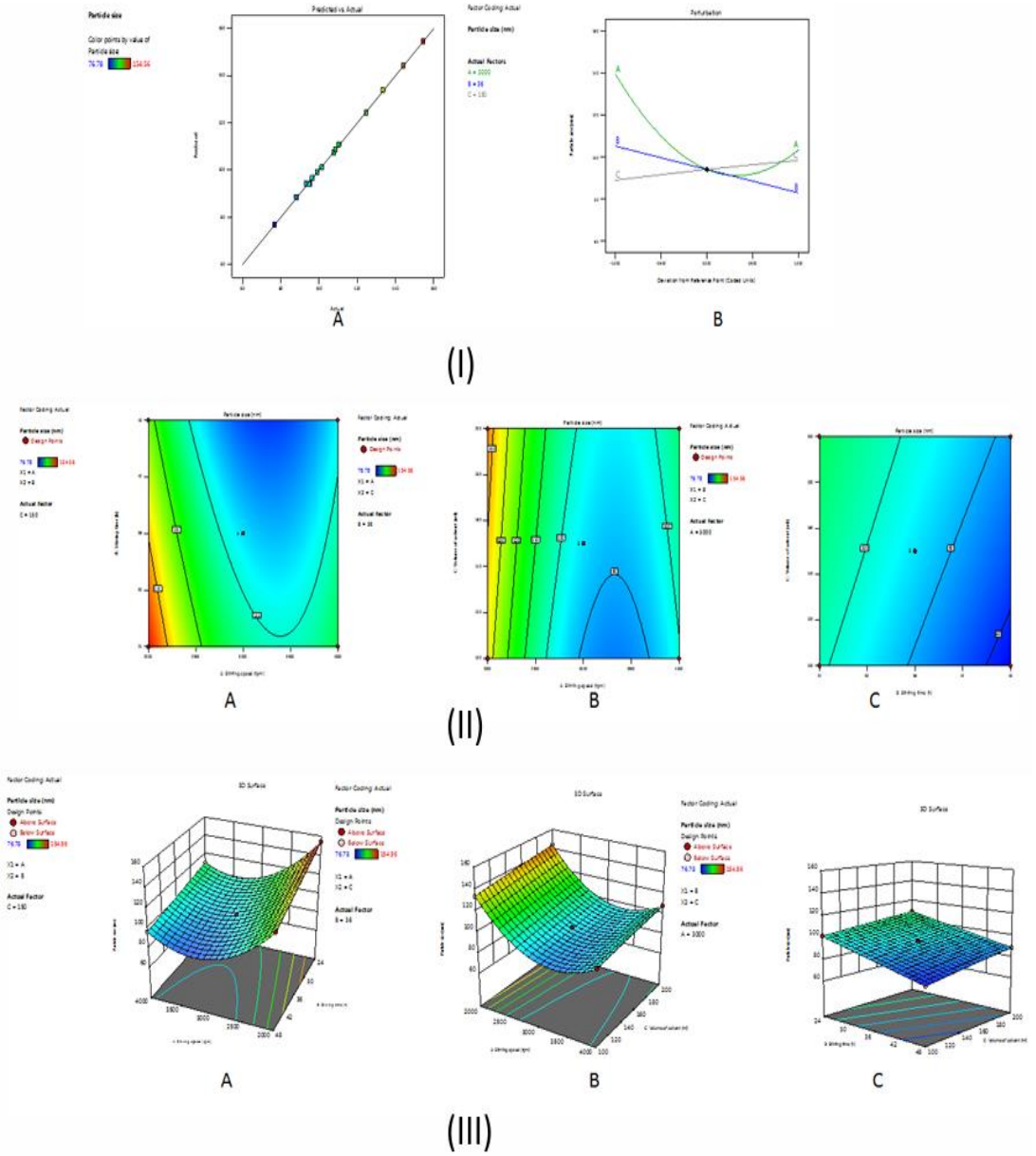

Fig. 1: I. (A) Comparison between predicted and actual values on mean particle size; (B) Perturbation plot displaying the effect of A, B and C on particle size. II and III. Contour and 3D response surface plots exhibit interactive effect between independent variables

Encapsulation efficiency

NS encapsulation may improve medication bioavailability and controlled release [29]. NS had 76.62% to 86.68% encapsulation efficiency. The polynomial model shows that parameters A, B, and C considerably affect encapsulation efficiency. Model significance was demonstrated by F-value 56.60. The model terms with P-values below 0.05 were significant. The model terms A, B, C, A^2, B^2, and C^2 were significant by P and F-values. The modified R^2 score of 0.9691 and anticipated R2 value of 0.9042 indicated model reliability. Analysing the signal-to-noise ratio 30.368 helps this model navigate design space. Precision determines the signal-to-noise ratio and should be greater than 4. A 30.368 ratio suggests a strong signal. Design may be navigated with this model. The equation showed that components A and B improve encapsulation efficiency, whereas factor C negatively affects it. Individual effects and perturbation plots compared expected and actual values and indicated the effects of A, B, and C on particle size (fig. 2(A) and 2(B)). The statistics clearly revealed that C has the greatest impact on encapsulation efficiency, followed by A and B. Fig. 2 shows how independent variables affect practical yield.

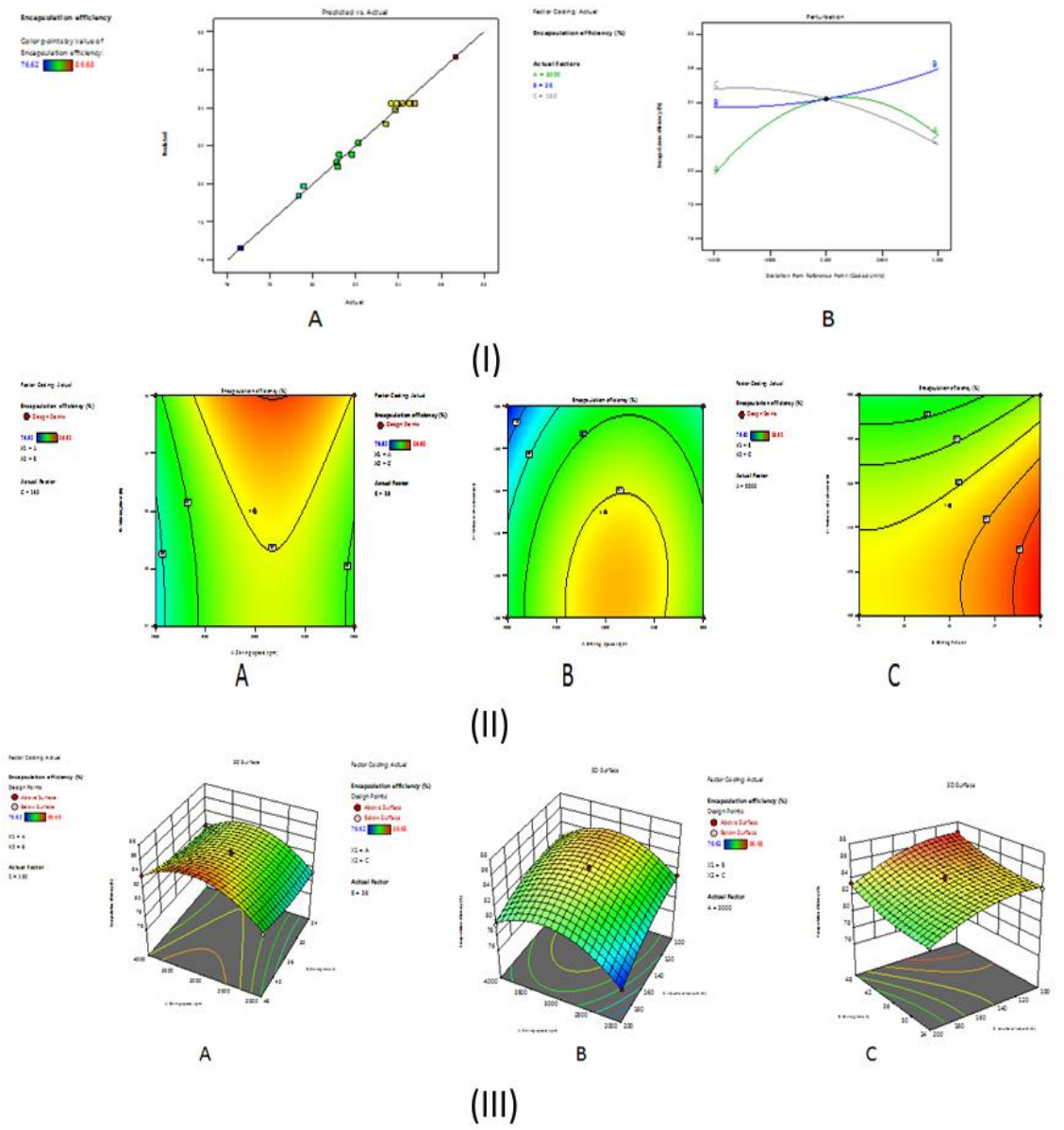

Fig. 2: I (A) The Comparison of predicted and actual values on Encapsulation efficiency; (B) Perturbation plot based on the effect of A, B and C on Encapsulation efficiency. IIandIII. Contour and 3D Response surface plots based on the interactive effect between independent variables

Optimization

Optimisation of selected variable-influenced response parameters used Derringer's desire function (D). The responses (mean particle size and encapsulation efficiency) formed a desirability scale. Each response's aim function (D) was Y_{max} and Y_{min}. Contour plots show the relationship between fitted responses for two components in each plot. The graph's darkest section showed ideal values. In fig. 3, 3D contour plots showed the relationship between two variables on X-and Y-axes and a response value on Z-axis.

Characterisation of plain β-CDNS and CUNS

CUNS had a low polydispersity index (0.194±0.005 to 0.236±0.005) and an average particle size of 70–80 nm. The particle size distribution's unimodality and narrow range. Low polydispersity indicates colloidal particle homogeneity [30]. With a high zeta

potential (-24.7±3.9 to-26.8±2.8mV), complexes should be stable and unlikely to agglomerate. Fine, free-flowing powders were found in all formulations. In fig. 4, TEM showed that drug encapsulation does not modify the spherical shape or size of plain NS. Drug loading in CUNS ranged from 36.86 to 38.46, and encapsulation percentages above 85%.

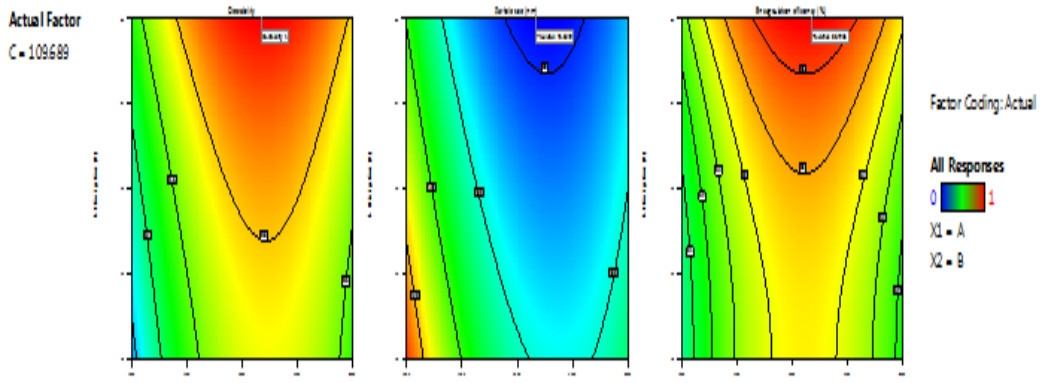

Fig. 3: 3D contour plots showing the relationship between two variables and a response

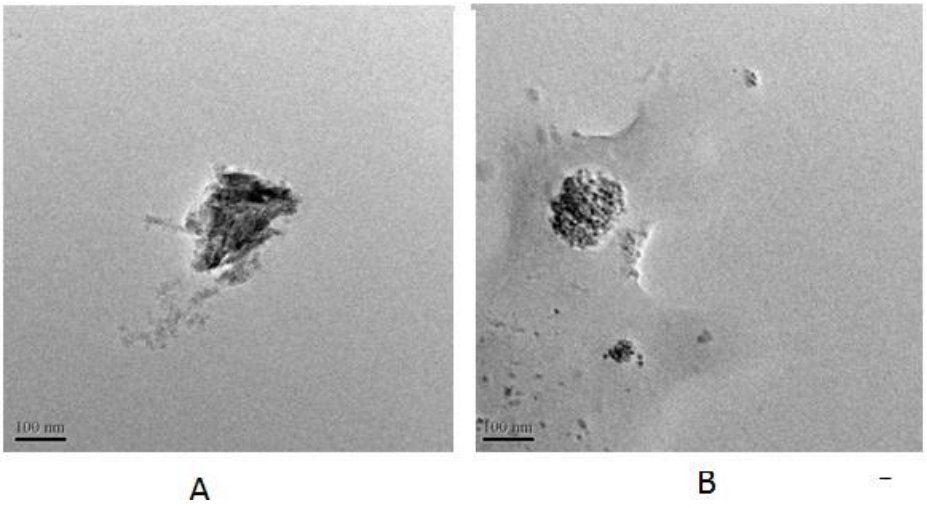

Fig. 4: TEM image of A. plain NS B. Curcumin loaded NS complexes

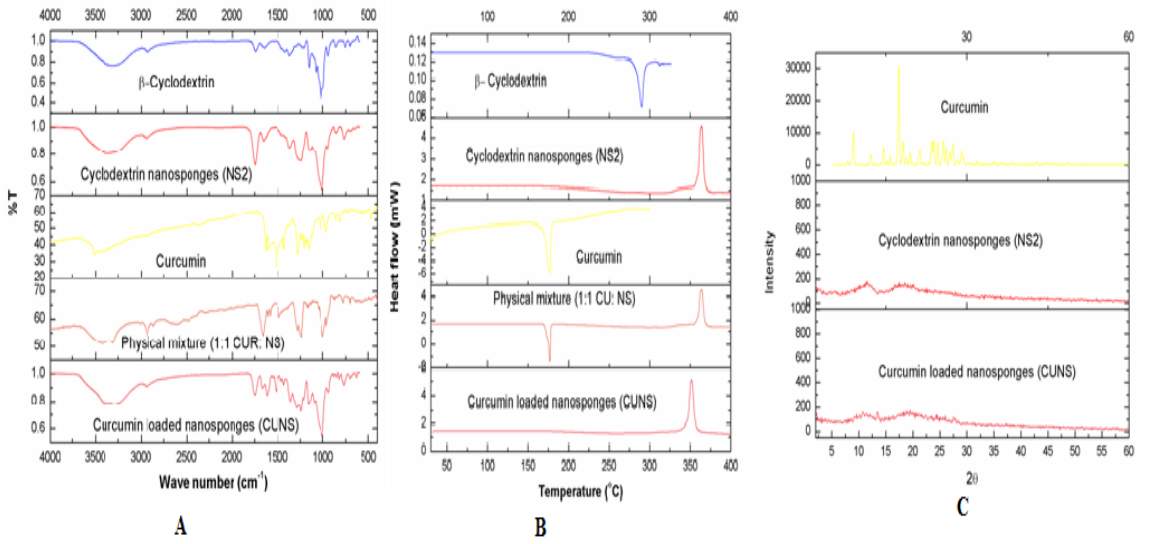

Fig. 5: (A) FTIR spectra of β-CD, plain NSs, Curcumin, Physical mixture and Curcumin loaded NSs; (B) DSC thermograms of β-CD, plain NSs, Curcumin, Physical mixture and curcumin-loaded NSs; (C) XRPD pattern of Curcumin, plain NSs and curcumin loaded NSs complexes

Fig. 5A displays FTIR spectra of β-CD, plain NS, CU, physical combination, and CUNS. The free drug's FTIR spectra showed characteristic peaks at 3510.56, 3421.83, 3014.84, 2850.88, 2366.74, 1627.97, 1602.90, 1510.31, 1429.30, 1280.78, 1153.47, 1026.16, 964.44, and 808.20 cm-1 The imidazole bond peak in plain NS, between 1740 and 1750 cm-1, confirms the formation of β-CDNS.

Additional characteristic NS peaks appeared at 1026 cm-1 from the primary alcohol's C-O stretching vibration, 1418 cm-1 from C-H bending vibration and 2918 cm-1 from C-H stretching vibration. The FTIR spectra investigation shows that the fingerprint region (900-1,400 cm−1) stays substantially unchanged, as shown in fig. 5A.

Fig. 5B shows CU, ß-cyclo dextrin, and CUNS DSC thermograms. The strong melting point at 176 °C suggested crystalline CU. Exothermic peak at 350 °C showed plain nano sponge thermogram because CU is less complicated. This may indicate that the formulation's components interact [31].

The XRD patterns of pure CU, plain NS, and CUNS were analysed to determine the physical characteristics of CU in β-CDNS. The x-ray diffract to gram of plain CU confirmed its crystal form with strong peaks at 2θ values of 11.28, 15.92, 17.12, 19.68, 23.03, 25.8, 26.015, 27.66, 29.16, and 41.27 (fig. 5C). The nano version of CU lacked its endothermic peak fig. 5C showed that CU's compound had no crystalline peak. These findings corroborate NSCU encapsulation. experimental examination like FTIR, DSC, and XRD confirms CU encapsulation in NS. An XRPD study [32] found that freeze-drying produces a fluffy, porous bulk powder without crystallinity.

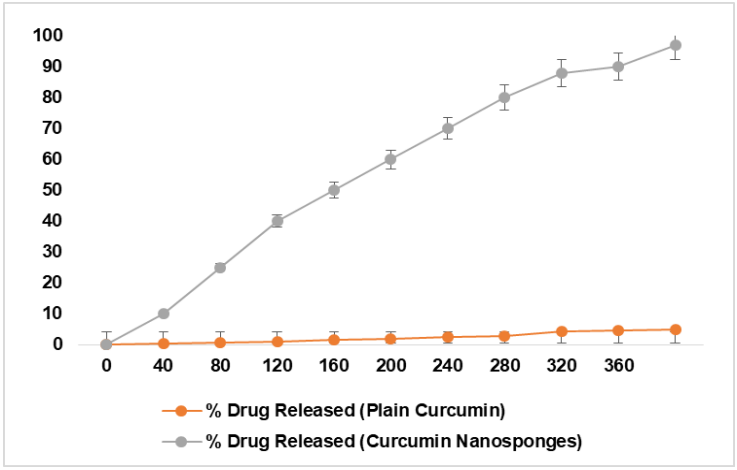

(A)

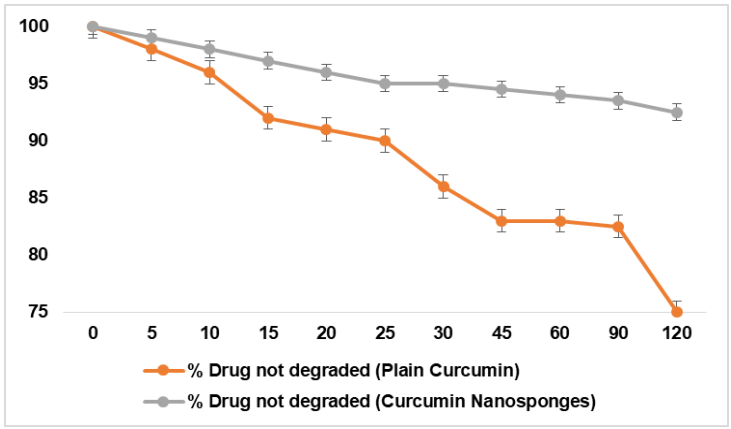

(B)

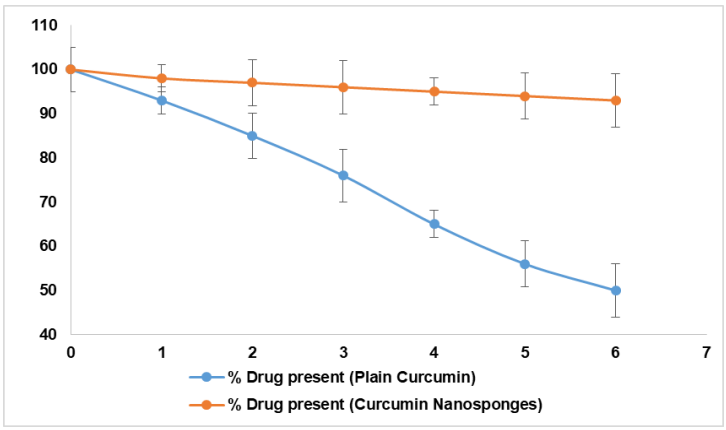

(C)

Fig. 6: (A) Dissolution profile of plain curcumin and curcumin loaded NS Photo stability studies (B) Photodegradation of plain curcumin and curcumin loaded NS (C) Stability of free and encapsulated curcumin within 6 h at 37 °C, All the values were expressed in mean±SD (n=3)

In simulated gastric medium, CU and CUNS dissolve as shown in fig. 6A. CU released from NS quickly and completely in *in vitro* experiments. NS release CU faster than pure CU, which takes 120 min to dissolve 3%. An average of 50% CU was released in 30 min, indicating a fast burst. Perhaps the fraction of CU encapsulated as a non-inclusion complex on the NS surface. After adding the formulation to the release medium, this drug immediately permeated the liquid. Nearly 90% of CU left the NS complex after 120 h. After the first impact, both formulations released slower [33].

Free and complexed CU were irradiated separately to measure photodegradation. (fig. 6B). CU without NS degrades faster than free CU. CU's strong NS encapsulation may explain this. CU from formulations deteriorated faster in the first 30 min. CU on NS may produce this [34]. In six hours, free CU fell by roughly 50% in simulated intestinal fluid, whereas the encapsulated versions, shown in fig. 6C, did not. Inclusion complexes are hypothesised to protect medications from the stomach [35].

Evaluation of CUNS tablets

These pills were evaluated for quality control characteristics. Tablets manufactured have a mean hardness of 4.78±0.72-5.66±0.39 kg/m^2. Hardness was consistent among F1–F10 tablets. Every pill composition gained strength and mechanical stress resistance. Tablet weight of the formulation ranged from 497.83±1.36 to 503.42±2.31 mg. No batch deviated from the tablet weight by more than 5%, demonstrating tablet formulation and manufacturing consistency. Tablets with drug content ranging from 98.82±2.66 to 102.56±1.78% revealed homogenous mixing, making all formulations acceptable. Every prepared tablet was compact and friable (less than 1%). Every tablet swelled in 15 min. After smoothing the tablet's jagged ends to leave a gel coating, water seeping through led it to lose some integrity and fluctuate in size. Every pill was well-hydrated. In swelling testing, tablets in formulations (F1–F6) containing hydroxypropyl methylcellulose (HPMC) polymer eroded, whereas tablets in formulations (F7, F8, F9) did not, probably because HPMC was absent. Formulations F7–F9 create a gel coating on the tablet. Tablet erosion was reduced in formulation F10 than in F1–F6. The F1 and F2 formulations showed improved *in vitro* release at 12 h, with 97.12±2.38 and 95.34±3.24 percent, respectively, according to drug release data. Wetting a CU-based nano tablet on sheep vaginal mucosa swells bio-adhesive polymers at the interface, causing molecular interaction at the mucus layer. HPMC and xanthum gum formulations had stronger bio adhesion than others, possibly due to secondary chemical interactions between polymer chains and mucin molecules. No formulation had higher bioadhesion than F2. Guar gum formulations had the lowest bioadhesion, possibly due to weak surface adhesive bonding. According to ex-vivo and bioadhesive experiments, formulations F2 and F1 had significant mucoadhesive times of 24.22 and 21.22 min, respectively. F2 and F1 have *ex vivo* bioadhseive times of 152 and 132. Based on findings, F2 and F1 performed well across all 10 formulations.

Histopathology showed that control mice had increased stromal vessel density and well-preserved epithelium, while endometriosis mice had leukocyte infiltration and fibrosis. However, CU-loaded nano tablets considerably improved these problematic characteristics. This supports research that amygdalin significantly lowers endometriosis pathology scores. Lesion alterations were considerable in the surgically induced endometriosis group. In the columnar epithelial layer and glands, endometrial destruction was greater. Endometrial lesion layers showed haemorrhage, vascular congestion, necrosis, inflammatory cell infiltration, cystically dilated glands, and blood cell accumulation in the lumen (fig. 7). All histological indicators improved after CU-loaded Nano pill intake.

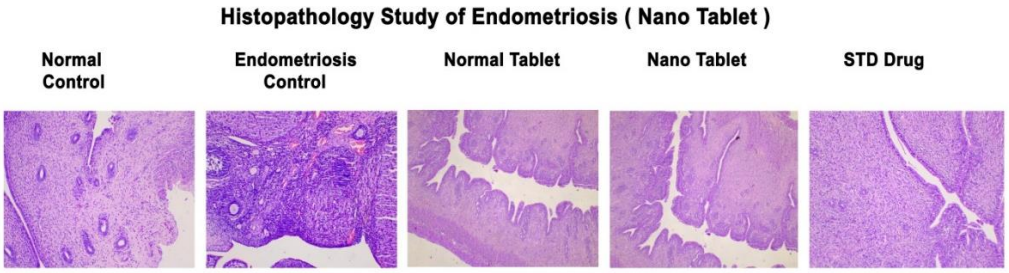

Fig. 7: Histopathology report on curcumin nanotablet

Future perspectives

Nanosponges are widely recognised as the leading medication delivery technology in the field of Pharmaceutics. Future research should prioritise the development of effective methods to modify nanosponges in order to decrease toxicity, enhance their selectivity, and improve their biosafety. It is possible to create nanosponges that are innovative, possess different features, and have multifunctionality. To create versatile systems with cancer theranostic capabilities, additional study is needed to focus on the precise surface modification of nanosponges using various materials, including fluorescent compounds and Magnetite nanoparticles. Utilising 3D printing technology facilitates the efficient and expeditious manufacturing of nanosponges.

CONCLUSION

CUNS were produced and extensively characterised utilising particle size analysis, FTIR spectroscopy, DSC, and XRD. These investigations indicated that CU was successfully encapsulated within the NS and formed an amorphous drug compound. According to the trial results, the nano tablets metal of the quality control parameters, including weight, thickness, hardness, friability, drug content, muco adhesive time, and bioadhesive time. The disintegration characteristic of the nano tablets showed a biphasic release system, with initial burst release followed by continuous release. The histopathology investigation also confirmed the protective effect of the CU-containing Nano pill. As a result, this study demonstrated the feasibility of using Nano tablets for targeted medication administration in endometriosis treatment.

ACKNOWLEDGEMENT

The authors express their gratitude to the administration and staff of DIT University, Dehradun, Uttarkhand, India and St Mary's College of Pharmacy, Secunderabad, Telangana, India, for their valuable support in allowing the research. The students are appreciative of the assistance and motivation they have received throughout their time at this establishment.

FUNDING

Nil

AUTHORS CONTRIBUTIONS

The research work and writing were completed by U. A. and reviewed and edited by G. M and B. K. All authors agree with the

submission and publication. Both have read and agreed to the published edition of the manuscript.

CONFLICT OF INTERESTS

The authors of this work have stated that they do not have any real, anticipated, or apparent conflicts of interest.

REFERENCES

1. Friend DR. Drug delivery for the treatment of endometriosis and uterine fibroids. Drug Deliv Transl Res. 2017 Dec;7(6):829-39. doi: 10.1007/s13346-017-0423-2, PMID 28828592.
2. Zhao Y, Gong P, Chen Y, Nwachukwu JC, Srinivasan S, KO C. Dual suppression of estrogenic and inflammatory activities for targeting of endometriosis. Sci Transl Med. 2015 Jan 21;7(271):271ra9. doi: 10.1126/scitranslmed.3010626, PMID 25609169.
3. Bina F, Soleymani S, Toliat T, Hajimahmoodi M, Tabarrai M, Abdollahi M. Plant-derived medicines for treatment of endometriosis: a comprehensive review of molecular mechanisms. Pharmacol Res. 2019 Jan;139:76-90. doi: 10.1016/j.phrs.2018.11.008, PMID 30412733.
4. Saltan G, Suntar I, Ozbilgin S, Ilhan M, Demirel MA, OZ BE. Viburnum opulus L. a remedy for the treatment of endometriosis demonstrated by rat model of surgically induced endometriosis. J Ethnopharmacol. 2016 Dec;193:450-5. doi: 10.1016/j.jep.2016.09.029, PMID 27647013.
5. Liu JP, Lewith G, Little P, LI Q. Chinese herbal medicine for endometriosis. Flower a. Cochrane Database Syst Rev. 2012 May;5:CD006568.
6. Sarfaraz MD, Shaikh ZM, Doddayya H. Preparation and characterization of fluconazole topical nanosponge hydrogel. Int J Pharm Pharm Sci. 2024 Apr;16(4):18-26. doi: 10.22159/ijpps.2024v16i4.50589.
7. Bhagyavathi A, Sai Lakshmi TK, Sahitya DM, Bhavani B. Nanosponges a revolutionary targeted drug delivery nanocarrier: a review. Asian J Pharm Clin Res. 2023 Apr;16(4):3-9.
8. Chilajwar SV, Pednekar PP, Jadhav KR, Gupta GJ, Kadam VJ. Cyclodextrin based nanosponges: a propitious platform for enhancing drug delivery. Expert Opin Drug Deliv. 2014 Jan;11(1):111-20. doi: 10.1517/17425247.2014.865013, PMID 24298891.
9. Pawar S, Shende P, Trotta F. Diversity of β-cyclodextrin based nanosponges for transformation of actives. Int J Pharm. 2019 Jun;565:333-50. doi: 10.1016/j.ijpharm.2019.05.015, PMID 31082468.
10. Shraddha T, Shashikant D, Tanuja U, Nilesh K. Cyclodextrin in novel formulations and solubility enhancement techniques: a review. Int J Curr Pharm Res. 2024 Feb;16(2):9-18. doi: 10.22159/ijcpr.2024v16i2.4032.
11. Hema AN, Gaayathri G, Gundeti S. Development of orodispersible tablets of loratadine containing an amorphous solid dispersion of the drug in soluplus® using design of experiments. Int J Pharm Pharm Sci. 2023 Aug;15(8):19-27.
12. Duggi VR, Ambati SR. Preparation and evaluation of nanosponges-based tramadol HCl c/r tablets using design of experiment. Int J Appl Pharm. 2022 Mar;14(3):86-94.
13. N Politis S, Colombo P, Colombo G, M Rekkas D. Design of experiments (DoE) in Pharmaceutical development. Drug Dev Ind Pharm. 2017 Jun;43(6):889-901. doi: 10.1080/03639045.2017.1291672, PMID 28166428.
14. Konda M, Sampathi S. QBD approach for the development of capsaicin loaded stearic acid grafted chitosan polymeric micelles. Int J App Pharm. 2023 Apr;15(4):131-42. doi: 10.22159/ijap.2023v15i4.48101.
15. JA, Girigoswami A, Girigoswami K. Versatile applications of nanosponges in the biomedical field: a glimpse on SARS-COV-2 management. Bionanoscience. 2022;12(3):1018-31. doi: 10.1007/s12668-022-01000-1, PMID 35755139.
16. Sadjadi S, Malmir M, Heravi MM, Raja M. Magnetic hybrid of cyclodextrin nanosponge and polyhedral oligomeric silsesquioxane: efficient catalytic support for immobilization of Pd nanoparticles. Int J Biol Macromol. 2019;128:638-47. doi: 10.1016/j.ijbiomac.2019.01.181, PMID 30708003.
17. Tejashri G, Amrita B, Darshana J. Cyclodextrin based nanosponges for pharmaceutical use: a review. Acta Pharm. 2013 Mar;63(3):335-58. doi: 10.2478/acph-2013-0021, PMID 24152895.
18. Vij M, Dand N, Kumar L, Wadhwa P, Wani SU, Mahdi WA. Optimisation of a greener approach for the synthesis of cyclodextrin-based nanosponges for the solubility enhancement of domperidone a BCS Class II drug. Pharmaceuticals (Basel). 2023 Apr;16(4):567. doi: 10.3390/ph16040567, PMID 37111324.
19. Singireddy A, Rani Pedireddi SR, Nimmagadda S, Subramanian S. Beneficial effects of microwave-assisted heating versus conventional heating in synthesis of cyclodextrin-based nanosponges. Mater Today Proc. 2016 Nov;3(10):3951-9. doi: 10.1016/j.matpr.2016.11.055.
20. Moretton MA, Cohen L, Lepera L, Bernabeu E, Taira C, Hocht C. Enhanced oral bioavailability of nevirapine within micellar nanocarriers compared with Viramune(®). Colloids Surf B Biointerfaces. 2014 Oct 1;122:56-65. doi: 10.1016/j.colsurfb.2014.06.046, PMID 25016545.
21. Madan JR, Kamate VJ, Dua K, Awasthi R. Improving the solubility of nevirapine using a hydrotropy and mixed hydrotropy based solid dispersion approach. Polim Med. 2017 Feb;47(2):83-90. doi: 10.17219/pim/77093, PMID 30009585.
22. Sinha D, DE D, Ayaz A. Performance and stability analysis of curcumin dye as a photosensitizer used in nanostructured ZnO based DSSc. Spectrochim Acta A Mol Biomol Spectrosc. 2018 Mar;193:467-74. doi: 10.1016/j.saa.2017.12.058, PMID 29289745.
23. Volpatti D, Gulisano E, Spanghero M. Short note: infliximab recovery in a simulated intestinal fluid of the upper intestine tract. Hum Antibodies. 2019 Apr;27(4):241-6. doi: 10.3233/HAB-190378, PMID 30958344.
24. Nagar P, Singh K, Chauhan I, Verma M, Yasir M, Khan A. Orally disintegrating tablets: formulation preparation techniques and evaluation. J Appl Pharm Sci. 2011 Jun;30:35-45.
25. Brandt K, Barrangou R. Adaptive response to iterative passages of five lactobacillus species in simulated vaginal fluid. BMC Microbiol. 2020 Jan;20(1):339. doi: 10.1186/s12866-020-02027-8, PMID 33172400.
26. Somigliana E, Vigano P, Vignali M. Endometriosis and unexplained recurrent spontaneous abortion: pathological states resulting from aberrant modulation of natural killer cell function? Hum Reprod Update. 1999 Jan;5(1):40-51. doi: 10.1093/humupd/5.1.40, PMID 10333368.
27. Anandam S, Selvamuthukumar S. Fabrication of cyclodextrin nanosponges for quercetin delivery: physicochemical characterization photostability and antioxidant effects. J Mater Sci. 2014;49(23):8140-53. doi: 10.1007/s10853-014-8523-6.
28. Singireddy A, Subramanian S. Cyclodextrin nanosponges to enhance the dissolution profile of quercetin by inclusion complex formation. Part Sci Technol. 2016 Mar;34(3):341-6. doi: 10.1080/02726351.2015.1081658.
29. Anandam S, Selvamuthukumar S. Optimization of microwave-assisted synthesis of cyclodextrin nanosponges using response surface methodology. J Porous Mater. 2014;21(6):1015-23. doi: 10.1007/s10934-014-9851-2.
30. Singireddy A, Pedireddi SR, Subramanian S. Optimization of reaction parameters for synthesis of cyclodextrin nanosponges in controlled nanoscopic size dimensions. J Polym Res. 2019 Nov;26:1-2.
31. Naysmith A, Mian NS, Rana S. Development of conductive textile fabric using plackett burman optimized green synthesized silver nanoparticles and in situ polymerized polypyrrole. Green Chem Lett Rev. 2023 Jan;16(1):2158690. doi: 10.1080/17518253.2022.2158690.
32. Tran PH, Tran TT. Encapsulation of lipid-based formulations in porous carriers for controlled drug delivery. Curr Med Chem. 2021;28(42):8711-21. doi: 10.2174/0929867328666210420103841, PMID 33881970.
33. Torisu T, Maruno T, Yoneda S, Hamaji Y, Honda S, Ohkubo T. Friability testing as a new stress stability assay for biopharmaceuticals. J Pharm Sci. 2017 Oct;106(10):2966-78. doi: 10.1016/j.xphs.2017.05.035, PMID 28603019.
34. Bayer IS. Controlled drug release from nanoengineered polysaccharides. Pharmaceutics. 2023 May;15(5):1364. doi: 10.3390/pharmaceutics15051364, PMID 37242606.
35. Sarvan VH, Vashisth H. Types and application of pharmaceutical nanotechnology: a review. Int J Curr Pharm Sci. 2023 Mar;15(3):14-8. doi: 10.22159/ijcpr.2023v15i3.3010.